Journal of Structural Geology 32 (2010) 1643–1655

Contents lists available at ScienceDirect

Journal of Structural Geology

journal homepage: www.elsevier.com/locate/jsg

Effects of internal structure and local stresses on fracture propagation, deflection, and arrest in fault zones

Agust Gudmundsson [a,*], Trine H. Simmenes [b,1], Belinda Larsen [b], Sonja L. Philipp [c]

[a] Department of Earth Sciences, Royal Holloway, University of London, Egham, Surrey TW20 0EX, UK
[b] Department of Earth Science, University of Bergen, Norway
[c] Geoscience Centre, University of Göttingen, Germany

ARTICLE INFO

Article history:
Received 12 April 2009
Received in revised form
1 August 2009
Accepted 20 August 2009
Available online 10 September 2009

Keywords:
Damage zone
Fault core
Crustal stresses
Toughness
Fractures
Crustal fluids

ABSTRACT

The way that faults transport crustal fluids is important in many fields of earth sciences such as petroleum geology, geothermal research, volcanology, seismology, and hydrogeology. For understanding the permeability evolution and maintenance in a fault zone, its internal structure and associated local stresses and mechanical properties must be known. This follows because the permeability is primarily related to fracture propagation and their linking up into interconnected clusters in the fault zone. Here we show that a fault zone can be regarded as an elastic inclusion with mechanical properties that differ from those of the host rock. As a consequence, the fault zone modifies the associated regional stress field and develops its own local stress field which normally differs significantly, both as regard magnitude and orientation of the principal stresses, from the regional field. The local stress field, together with fault-rock heterogeneities and interfaces (discontinuities; fractures, contacts), determine fracture propagation, deflection (along discontinuities/interfaces), and arrest in the fault zone and, thereby, its permeability development. We provide new data on the internal structure of fault zones, in particular the fracture frequency in the damage zone as a function of distance from the fault core. New numerical models show that the local stress field inside a fault zone, modelled as an inclusion, differ significantly from those of the host rock, both as regards the magnitude and the directions of the principal stresses. Also, when the mechanical layering of the damage zone, due to variation in its fracture frequency, is considered, the numerical models show abrupt changes in local stresses not only between the core and the damage zone but also within the damage zone itself. Abrupt changes in local stresses within the fault zone generate barriers to fracture propagation and contribute to fracture deflection and/or arrest. Also, analytical solutions of the effects of material toughness (the critical energy release rate) of layers and their interfaces show that propagating fractures commonly become deflected into, and often arrested at, the interfaces. Generally, fractures propagating from a compliant (soft) layer towards a stiffer one tend to become deflected and arrested at the contact between the layers, whereas fractures propagating from a stiff layer towards a softer one tend to penetrate the contact. Thus, it is normally easier for fractures to propagate from the host rock into the damage zone than vice versa. Similarly, it is easier for fractures to propagate from the outer, stiffer parts of the damage zone to the inner, softer parts, and from the stiff host rock to the outer damage zone, than in the opposite directions. These conclusions contribute to increased understanding as to how fractures propagate and become arrested within fault zones, and how the fault zone thickness is confined at any particular time during its evolution.

1. Introduction

In recent years, there has been considerable geological work on the internal structure of major fault zones (e.g., Byerlee, 1993; Bruhn et al., 1994; Caine et al., 1996; Sibson, 1996; Evans et al., 1997; Gutmanis et al., 1998; Sibson, 2003; Gudmundsson, 2004; Shimamoto et al., 2004; Berg and Skar, 2005; Agosta and Aydin, 2006; Faulkner et al., 2006; Bradbury et al., 2007; Li and Malin, 2008). This work has partly focused on analysing the fault rocks themselves,

* Corresponding author.
E-mail addresses: a.gudmundsson@es.rhul.ac.uk, rock.fractures@googlemail.com (A. Gudmundsson).
[1] Present address: StatoilHydro Research Center, Sandsliveien 90, 5020 Bergen, Norway.

0191-8141/$ – see front matter © 2009 Elsevier Ltd. All rights reserved.
doi:10.1016/j.jsg.2009.08.013

Fig. 1. View west, two parallel fault zones seen as lineaments (marked by arrows) dissecting layers of limestone and shale in the Bristol Channel at Kilve, the Somerset Coast, England. The distance between the faults at the location of the arrows is about 25 m.

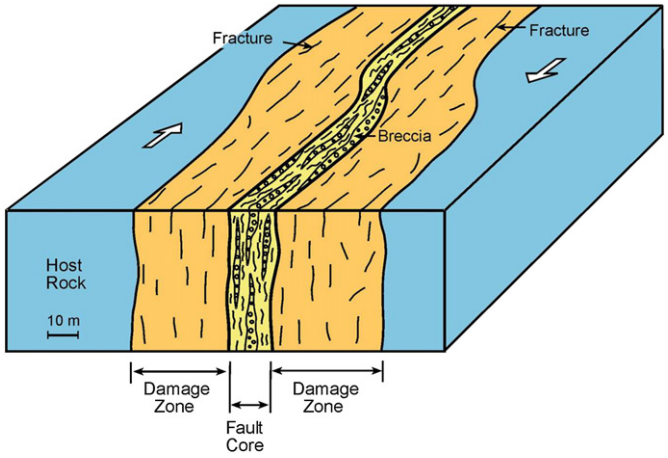

Fig. 2. Schematic illustration of a fault core and fault damage zone of a (strike-slip) fault. The core consists primarily of breccia and cataclastic rock (Fig. 3). The damage zone, located on each side of the core, commonly contains some cataclastic rocks and breccias but is characterised by numerous faults and fractures (Figs. 5 and 8), many of which are eventually filled with secondary minerals (Fig. 4).

their structure and mechanical properties, and partly on the permeability structure and its maintenance in fault zones. This is because of the importance that fluid transport by fault zones has in many fields of earth sciences. In particular, the in situ bulk hydraulic characteristics of fault zones have been measured in boreholes (e.g., Ahlbom and Smellie, 1991; Barton et al., 1995; Fisher et al., 1996; Braathen et al., 1999; Nativ et al., 1999; Lin et al., 2007; Tanaka et al., 2007) and modelled (e.g., Barton et al., 1995; Lopez and Smith, 1995; Bredehoeft, 1997; Faulkner et al., 2006; Healy, 2008; Li and Malin, 2008), the results suggesting that during non-slip periods the damage zone is the main conductor of fluids (cf. Gudmundsson, 2000; Gudmundsson et al., 2002).

Despite this work, the mechanical and permeability properties of major fault zones, including associated fracture propagation in the damage zone, are still not well understood, making it difficult to construct realistic numerical models. This is partly due to major fault zones being mechanically heterogeneous and, commonly, layered parallel with the fault plane. Thus, Young's modulus of a fault zone is likely to vary significantly with distance from the fault plane itself, that is, from the core and through the various subzones of the damage zone to the host rock (Gudmundsson, 2004; Gudmundsson and Brenner, 2003; Faulkner et al., 2006). As a consequence, fault zones tend to develop local stresses, many of which may be widely different from the associated regional stress fields (Gudmundsson and Brenner, 2003). Variations in local stresses are, in fact, universal features of mechanically layered rocks, whether the layering is parallel with the fault plane, and thus often steeply dipping or vertical, or gently dipping or horizontal as is many sedimentary basins and composite volcanoes (Gudmundsson, 2006; Gudmundsson and Philipp, 2006). In a fault zone, the local stress fields largely determine the fracture propagation and arrest, and associated seismic events, and thereby much of the fault-zone permeability.

This paper is on the internal mechanical structure of fault zones and how it affects local stresses, fracture development and arrest. The implications for fault-zone permeability are briefly discussed, but the focus is on the solid-mechanical aspects. In particular, the paper has three main aims. The first is to present results on the internal structure of fault zones and how they function as general elastic inclusions. The results derive from field studies of fault zones of various types. A second aim is to present new numerical models on the local stresses in fault zones. These models use field observations of internal structures of fault zones as a basis, focusing on the effects that different fracture frequencies have in generating subzones with different mechanical properties and local stresses within the main fault zones. The third aim is to explore the reasons why most fractures in fault zones remain short in comparison with the strike dimension of the fault zone itself. The explanation offered here is that the heterogeneous and anisotropic mechanical properties and local stresses within such fault zones, together with numerous interfaces/discontinuities (contacts, existing fractures), tend to deflect and, commonly, arrest most of the fractures after comparatively short propagation.

2. Internal structure of a fault zone

From a distance, fault zones appear as lineaments (Fig. 1). Indeed, fault zones are commonly viewed as lineaments with little or no internal structure and heterogeneity. As a consequence, fault zones have for a long time been modelled as single, elastic cracks or dislocations (Steketee, 1958; Press, 1965). While simple crack models can be very useful for understanding fault–fault interaction and fault effects on regional stresses, they are less useful for understanding the local stresses around and within the fault zone itself. Since these local stresses largely control the slip and fracture development and thus the permeability of the fault zone, the internal mechanical structure of the fault zone must be considered with a view of understanding its fluid-transport properties.

Detailed field observations of well-exposed fault zones show that they normally consist of two main structural units, namely a fault core and a fault damage zone (Fig. 2). The core takes up most of the fault displacement and it is also referred to as the fault slip zone (Bruhn et al., 1994; Sibson, 2003). Although the core contains many small faults and fractures, its characteristic features are breccias and cataclastic rocks. Commonly, the core rock is crushed and altered into a porous material (Fig. 3) that behaves as ductile or semi-brittle except at very high strain rates such as during seismogenic faulting. In the core, there are commonly numerous veins filled with secondary minerals spaced at centimetres or millimetres, that form dense networks. These networks, when transporting fluids, give the core a granular-media structure at the millimetre or centimetre scale, thereby supporting its being modelled as a porous medium.

While the field description in this paper of the fault core and damage zone focus on large fault zones, it should be emphasised

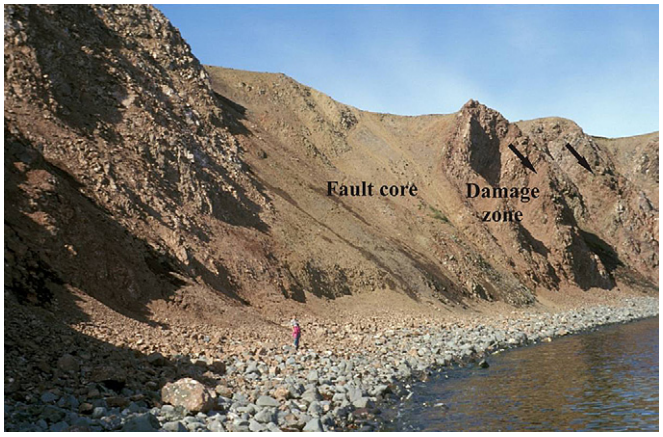

Fig. 3. Fault core and damage zone of a part of the Husavik-Flatey Fault, a transform fault partly exposed on land in North Iceland (Gudmundsson, 2007). View west, the 10-m-thick core (see the person for scale) strikes N62°W and is mainly of breccias (crushed basaltic lava flows), whereas the damage zone is characterised by tilted lava flows (dipping 40°NW) and fractures of various sizes and types, many of which are filled with secondary minerals (Fig. 4). Only a small part of the damage zone (which is many hundred metres thick) is seen in the photograph.

that the same units are seen in much smaller fault zones. In fact, laboratory experiments on small rock samples may produce very similar units, that is, a thin core and a thicker damage zone where the frequency of fractures changes irregularly, but generally decreases, with increasing distance from the core (Shimada, 2000).

In major fault zones, the thickness of the core is commonly from several metres to a few tens of metres (Fig. 3; Gudmundsson, 2004; Berg and Skar, 2005; Agosta and Aydin, 2006; Tanaka et al., 2007; Li and Malin, 2008). Very large faults zones, such as many transform faults, may, however, develop several fault cores and damage zones (Faulkner et al., 2006; Gudmundsson, 2007). The overall permeability of the core is very low during most of the interseismic (non-slip) period, so that the core commonly acts as a barrier to fluid flow, except during periods of high strain rates such as are associated with fault slip (Gudmundsson, 2000).

The damage zone, also referred to as the transition zone (Bruhn et al., 1994), consists partly of lenses of breccias and other heterogeneities, and partly of sets of extension fractures, and to a lesser degree, shear fractures (Gudmundsson et al., 2002). Many, and presumably most, of the extension fractures are hydrofractures that eventually become mineral-filled veins (Fig. 4). The fractures and faults, and other discontinuities, generally make the damage zone much more permeable than the fault core. For example, laboratory measurements indicate that hydraulic conductivities in the damage zone are as much as several orders of magnitude greater than those of either the fault core or the host rock (Evans et al., 1997; Seront et al., 1998).

Fig. 4. Mineral-vein network in a part of the damage zone of the Husavik-Flatey Fault (Fig. 3). Some 80% of the veins are pure extension fractures, driven open by fluid overpressure (Gudmundsson et al., 2002).

Fig. 5. View southeast, an example of the variation in fracture frequency with distance from the core of a fault in Vaksdal, West Norway. The highest number of fractures is at the contact between the core and the innermost part of the damage zone. From there, the fracture number decreases, in an irregular fashion, towards the host rock (gneiss), at about 10 m from the core. Many fracture frequency profiles of this type are provided by Simmenes (2002) and Larsen (2002).

There is normally not a sharp boundary between the damage zone and the host rock. In the host rock, also referred to as the protolith (Bruhn et al., 1994; Seront et al., 1998), the number of fractures is generally less than that in the damage zone (Fig. 5; Shimada, 2000). Although the boundaries between the fault core and the damage zone are sharper than those between the damage zone and the host rock, all these boundaries vary along the length of the fault and change, in time and space, with the evolution of the fault zone (Figs. 2 and 6).

Some general results of recent studies on the hydromechanical properties of the fault core, the damage zone, and the host rock may be briefly summarised as follows. The damage zone is the main conduit for flow of water along a major fault zone. Laboratory measurements of small samples indicate a permeability of the damage zone as much as 10,000-times higher than that of the core or the host rock. Evans et al. (1997) suggest that while the laboratory samples from the core yield hydraulic conductivity values that may not be much lower than the bulk in situ values, the laboratory values of hydraulic conductivity for the damage zone are likely to be considerably lower than the corresponding bulk in situ values. This follows because the larger, highly conductive fractures that are common in the damage zone (Figs. 4 and 5) are not represented in the small, relatively non-fractured laboratory samples. This conclusion is supported by reported in situ measurements giving fault zone permeabilities as much as 1000-times greater than the maximum laboratory values of Evans et al. (1997). Thus, the in situ permeability difference between the core and the damage zone may be even greater than the cited laboratory values would indicate.

3. Local stresses in fault zones

From a mechanical point of view, a fault zone may be regarded as an elastic inclusion (Fig. 6). As defined here, an elastic inclusion is

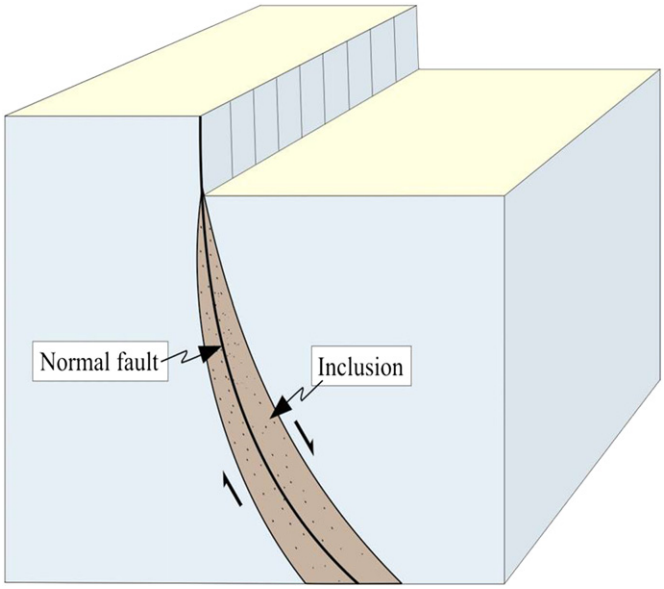

Fig. 6. Schematic illustration of a fault zone as an elastic inclusion (inhomogeneity). Normally, the elastic properties of the fault rock (damage zone and core) differ from those of the host rock, so that there will be stress concentration around the fault zone, as well as a local stress field inside it. It is this local stress field that controls fracture development and fault slip in the fault zone and, therefore, largely its permeability.

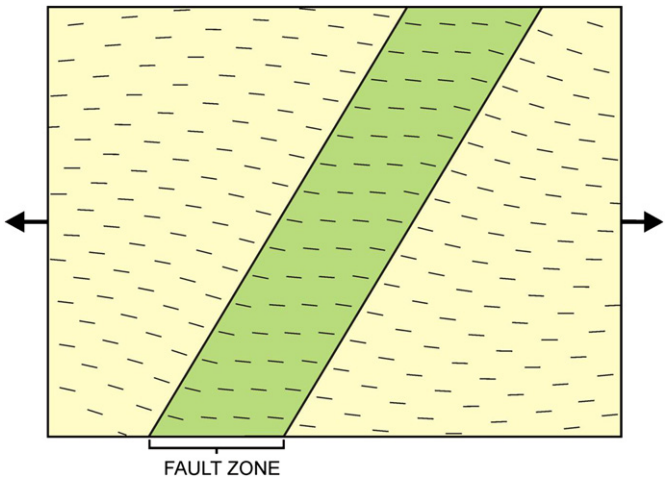

Fig. 7. Fault zone modelled as a simple elastic inclusion (Fig. 6). The finite-element (www.Ansys.com; Zienkiewicz, 1977) model can be viewed either as a sinistral strike-slip fault (lateral section) or as a normal fault (vertical section). Young's modulus of the fault zone is 1 GPa, a typical generalised value (Figs. 10 and 11), and that of the host rock 40 GPa. The horizontal tension is 5 MPa, a value close to the maximum tensile strength of solid rocks (Haimson and Rummel, 1982; Schultz, 1995; Amadei and Stephansson, 1997), and may thus be regarded as a typical loading before fault slip in active rift zones. The trends of the stress trajectories of σ_3 (the minimum principal compressive, maximum tensile, stress) change at the contact between the fault zone and the host rock, indicating that the fault zone has a local stress field different from the regional field of the host rock.

a three-dimensional body with elastic properties that differ from those of the host material. More specifically, an elastic inclusion is a body with material properties that contrast with those of the surrounding material, commonly referred to as the matrix, to which the inclusion is welded.

The concept of an elastic inclusion as described here is well established in the classical elasticity and rock mechanics literature (Eshelby, 1957; Savin, 1961; Jaeger et al., 2007). The more recent literature on micromechanics, however, uses "inhomogeneities" rather than elastic inclusions for the concept defined above (Nemat-Nasser and Hori, 1999; Qu and Cherkaoui, 2006). Here an elastic inclusion denotes a material body hosted by a larger body with different elastic properties (Gudmundsson, 2006), so that any rock body, such as a fault zone, hosted by a larger body with different properties is regarded as an inclusion.

The presence of an elastic inclusion modifies the regional stress field so as to generate a local stress field that operates both within the inclusion and in its vicinity (Fig. 7). This follows because the elastic properties of the inclusion, particularly its Young's modulus or stiffness, differ from those of the host rock. Thus, during any loading (stress, displacement, or pressure), the responses of the rocks constituting the inclusion differ from those of the surrounding rocks. For example, if the rocks that constitute the inclusion (the fault zone) are stiffer (higher Young's modulus) than the host rock, then the inclusion takes on most of the loading and becomes subject to either relative tensile stresses (if the loading is in extension) or compressive stresses (if the loading is in compression). By contrast, if the inclusion rocks are more compliant or softer than the host rock, then most of the loading is taken up by the host rock which, thereby, develops locally high relative tensile or compressive stresses depending whether the loading is in extension or compression.

As is indicated above, many, and perhaps most, fault zones are composed of a core and a damage zone that are widely different in mechanical properties (Figs. 2–5). In addition, the damage zone itself is commonly composed of subzones with different mechanical properties, partly attributable to variations in fracture frequencies (Figs. 5 and 8). Thus, the local stresses are likely to vary not only between the host rock and the fault zone, or between the core and the damage zone, but also within the damage zone itself.

To take the difference in stiffness between the host rock and the fault zone into account, and how these change the local stresses of fault zones, consider first the model in Fig. 9. This model is based on a normal fault zone in Vaksdal, close to Bergen in West Norway (Fig. 8). The model divides the fault zone into four main subzones. In the centre there is the fault plane itself, modelled as an internal, compliant elastic spring. Based on estimates from open fractures

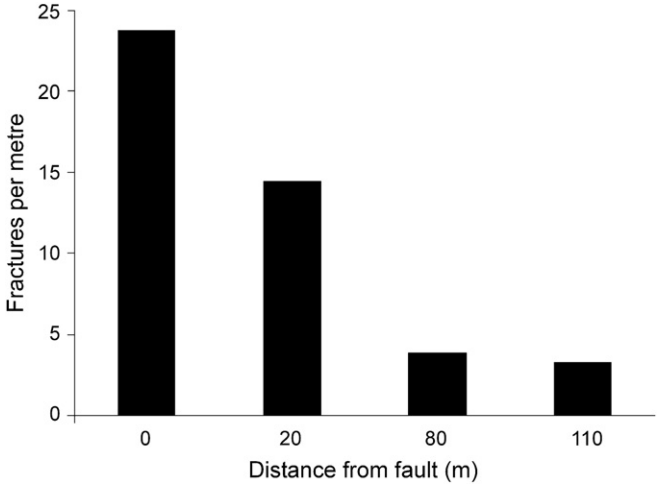

Fig. 8. Fracture frequency as a function of distance from the core of the fault modelled in Figs. 9 and 10. The measurements are from a major normal fault zone in Vaksdal, close to Bergen in West Norway (Simmenes, 2002). The inner part of the damage zone has 24 fractures per unit area but at a distance of 20 m from the core, the outer part of the damage zone has 14 fractures per unit area. Then at 80 m from the core, the fracture frequency has fallen to 4 per unit area and is the same at a distance of 110 m; these two latter areas are thus regarded as part of the host-rock fracture frequency.

Fig. 9. Set-up of the model in Fig. 10 is largely based on the internal structure of the fault zone in Fig. 8. The fault trends N40°E and is hosted by gneiss. The loading is E–W compressive stress of magnitude 15 MPa, as inferred from stress data from Norway (Hicks, 1996). The fault plane (the fracture represented by a red, thick line) has a stiffness of 6 MPa m^{-1}. The core has a Young's modulus of 0.1 GPa, the inner damage zone 1 GPa, the outer damage zone 10 GPa, and the host rock 50 GPa. The model is fastened in the corners (indicated by crosses) so as to avoid rigid-body rotation and translation (Simmenes, 2002).

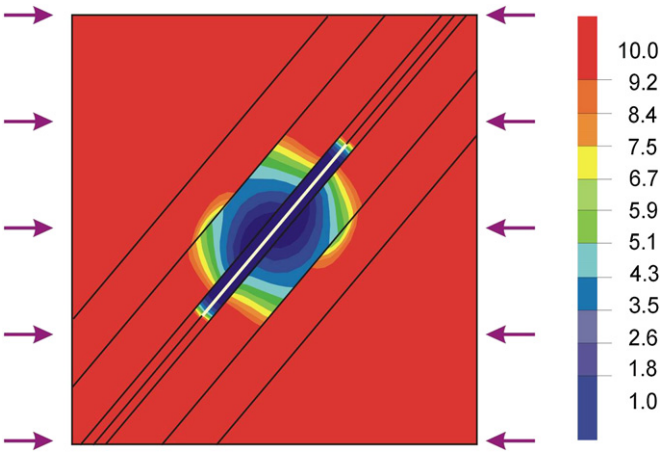

Fig. 10. Boundary-element (Beasy, 1991) model showing the von Mises shear-stress concentration (in MPa) around the fault zone in Fig. 9. The white line represents the fault plane. Clearly, the fault core and inner damage zone have comparatively low shear stress, 1–5 MPa, although high enough for slip, whereas the outer damage zone has comparatively high shear stress. The "stress transfer" from the stiffer parts of the damage zone, and into the host rock, is one way by which fault zones may grow (through fracture formation) in thickness over time.

(Gudmundsson and Brenner, 2003), the stiffness of the spring is taken as 6 MPa m^{-1}. The stiffness of an elastic spring is determined from a stress–displacement curve, whereas Young's modulus is determined from a stress–strain curve. Thus, while Young's modulus has the units of (M)Pa, the spring has the units of (M)Pa m^{-1}.

The fault plane is surrounded by the fault core, whose Young's modulus is taken as 0.1 GPa. This value is based on typical Young's moduli of unconsolidated rocks as well as in situ measurements from various fault cores worldwide with common values between 0.1 and 1 GPa (Hoek, 2000; Schon, 2004). The Young's modulus of the inner damage zone is 1 GPa, that of the outer damage zone 10 GPa, and that of the host rock 50 GPa. These values reflect the decreasing number of fractures (Fig. 8) with increasing distance from the inner damage zone to the host rock. The rock itself is gneiss, but in accordance with well-known effects of fractures and other cavities on Young's modulus (Farmer, 1983; Priest, 1993; Nemat-Nasser and Hori, 1999; Sadd, 2005), Young's modulus is low for the highly-fractured inner damage zone (Fig. 9), somewhat higher for the less-fractured outer damage zone, and highest for the normally fractured host rock.

The stress–concentration results (Fig. 10) indicate that, because of the lower Young's modulus inside the fault zone than outside it, for the given loading conditions there will be lower von Mises shear stresses in the fault zone than in the host rock. This may seem surprising given that, when generalised, the fault slip is mostly confined to the fault zone rather than the host rock. However, the von Mises shear stresses reach the typical stress drops/driving stresses for seismogenic fault slip, which are mostly 1–12 MPa (Scholz, 1990), and the slip would occur in the fault zone simply because it already has a weak fault plane and, most likely, a much higher pore-fluid pressure than the host rock. It is well-known that tectonic earthquakes are usually related to zones of high-fluid pressure, so that, using the modified Coulomb criterion, the driving shear stress for seismogenic fault slip, τ, becomes:

$$\tau = 2T_0 + f(\sigma_n - P) \quad (1)$$

where T_0 is the tensile strength of the rock, f is the coefficient of internal friction, σ_n is the normal stress on the fault plane, and P is the total fluid pressure on the fault plane at the time of slip. When the fluid pressure approaches or equals the normal stress, the term $f(\sigma_n - P)$ approaches or equals zero (for a higher fluid pressure the term may, in fact, become negative), so that the driving shear stress for slip becomes $2T_0$. Since the in situ tensile strength of rocks is commonly in the range of 0.5–6 MPa (Haimson and Rummel, 1982; Schultz, 1995; Amadei and Stephansson, 1997), it follows that, for high-fluid-pressure fault zones, the driving shear stress for slip should be 1–12 MPa, which is in agreement with common stress drops (Kasahara, 1981; Scholz, 1990). Thus, even if the low-Young's modulus in the damage zone and core results in comparatively low shear stresses in many active fault zones, they tend to slip because of the existing weak fault plane (or planes), the high-fluid-pressure (and thus low friction), and the low effective normal stress on the fault plane.

The local stresses in a fault zone do not depend only on the stress magnitudes, but also on the directions of the stress vectors, as represented by the trajectories of the principal stresses. The model in Fig. 7 considers the fault as a single zone, an inclusion, but as we have seen (Figs. 2–5, 8) there is commonly a significant difference in mechanical properties between the core and the damage zone, as well as between the various subzones of the damage zone itself. This is taken into account in the model in Fig. 10, and also in the model below (Fig. 11).

In the model in Fig. 11 the fault zone is divided into five subzones. One, in the centre, represents the core of the fault zone and has a Young's modulus of 1 GPa, similar to many compliant or soft breccias and unconsolidated rocks (Hoek, 2000; Schon, 2004). Then comes the inner part of the damage zone, on either side of the core, with a Young's modulus of 5 GPa. This is, again, similar to the Young's modulus of many fractured rocks, as is indicated above. The other part of the damage zone has a stiffness of 10 GPa, which is similar to many fractured rocks where the fractures are not very dense (Gudmundsson and Brenner, 2003). Finally, the host rock has a Young's modulus of 40 GPa, which is typical for many solid rocks (Bell, 2000; Nilsen and Palmström, 2000).

The loading is extension oblique to the fault (Fig. 11). Viewed in a vertical section, the loading would be appropriate for a reverse fault, whereas viewed in a lateral section, the loading would be appropriate for a dextral strike-slip fault. In either case, the oblique loading combined with the variation in stiffness (Young's modulus) towards the centre of the fault (through the damage zone and to the

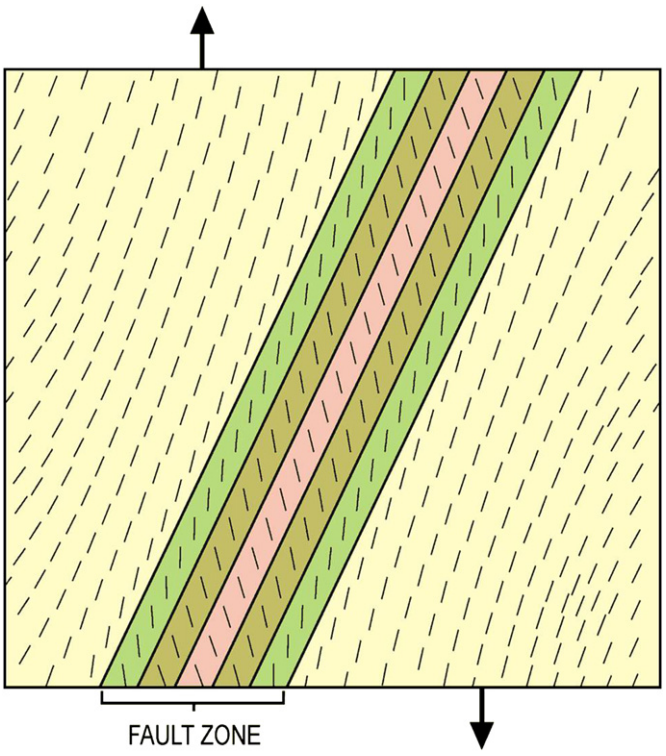

Fig. 11. Finite-element (www.Ansys.com; Zienkiewicz, 1977) model of the stress trajectories of σ_3 (the minimum principal compressive, maximum tensile, stress) in a fault zone composed of a core with a Young's modulus of 1 GPa, an inner damage zone with a Young's modulus of 5 GPa, and an outer damage zone with a Young's modulus of 10 GPa and located in a host rock with a Young's modulus of 40 GPa. The fault zone is subject to oblique loading, a tensile stress of 5 MPa. The trends of σ_3 differ between the core and the damage zone and the damage zone and the host rock, as well as between the subzones of the damage zone. This model demonstrates the variation in the local stresses that may occur within a typical "layered" fault zone.

core) results in rotation of the principal stresses. Rotations of the principal stresses within a fault zone are observed in the field, and are partly reflected in the different trend of fractures close to the fault plane or the core and away from the fault plane (in the damage zone). One such example is provided by a fault in the Bristol Channel of the UK (Fig. 12).

Models indicate that rotation of principal stresses is common in layered rocks, whether the layers are subhorizontal, inclined, or subvertical (Gudmundsson, 2006; Gudmundsson and Brenner, 2004; Faulkner et al., 2006; Gudmundsson and Philipp, 2006). Rotation of the principal stresses between layers of different mechanical properties is also common in the field outside fault zones, and is well demonstrated by changes in the orientation of extension fracture (joints, mineral veins) between the layers (Fig. 13).

The principal conclusion is that the fault zone develops a local stress field that controls its mechanical behaviour, slip, and permeability. Because of the mechanical layering inside the fault zone, the local stresses will vary between its subzones and, as a consequence, there will rarely be uniform stresses over large parts of the fault zone. It follows that stress field homogenisation over extensive parts of the fault zone, a necessary condition for large-scale fault slip (Gudmundsson and Homberg, 1999), is only rarely reached. Thus, most fault slips, both along the main fault itself as well as along smaller faults in the damage zone, remain small. Because of the variations in local stresses and rock properties, stress fields favouring a particular type of fracture propagation (such as a normal fault) are usually only reached within a comparatively small region within a single subzone of the fault zone. It follows that as soon as the particular fracture tries to propagate beyond that stress-homogenised region, the fracture enters regions that commonly have unfavourable local stresses, so that the fracture propagation becomes deflected and, often, arrested.

4. Fracture deflection and arrest

Most fractures propagate for only very short distances before they become arrested. This applies to crustal fractures in general, and fractures within the damage zones of fault zones in particular. The following terms are frequently used in the discussion below: a discontinuity, a contact, and an interface. The last one, interface, is the standard term in materials science for a contact between dissimilar (or similar) material layers or phases (solid, gas, liquid) (Sutton and Balluffi, 1995). In earth sciences, a contact between similar or dissimilar rocks has essentially the same meaning, whereas a discontinuity denotes a contact or a fracture with a negligible tensile strength (Priest, 1993). These terms will be used as appropriate, with interface being the most general one.

When a propagating fracture meets an interface or a discontinuity, such as a weak or open contact between dissimilar rocks or an earlier fracture, the propagating fracture may do one of the following (Fig. 14):

- become arrested so as to stop its propagation;
- penetrate the discontinuity;
- become deflected along the discontinuity, in one or two directions.

These three scenarios are well-known from field observations of rock fractures. Here we propose that fracture deflection at a discontinuity, as well as fracture arrest, can be understood in terms of three related parameters, namely:

- the induced tensile stress ahead of the propagating fracture tip;
- rotation of the principal stresses at the discontinuity;
- the material toughness or critical energy release rate of the discontinuity in relation to that of the adjacent rock layers.

4.1. Local stresses at a discontinuity

For a homogeneous, isotropic material the fracture-induced tensile stress ahead of and parallel to a propagating mode I crack, an extension fracture such as are common in fault zones (Fig. 4; Gudmundsson et al., 2002), is about 20% of the tensile stress ahead of and perpendicular to the crack (Cook and Gordon, 1964; Thouless and Parmigiani, 2007). Thus, the tensile stress induced by a fracture may open up a discontinuity ahead of the fracture tip if the tensile strength of the discontinuity is less than about 20% of the fracture-perpendicular tensile strength of the adjacent rock layers. For an average in situ rock tensile strength, 2–3 MPa (Haimson and Rummel, 1982; Schultz, 1995; Amadei and Stephansson, 1997), the discontinuity thus opens up if its tensile strength is less than 0.4–0.6 MPa. Since the minimum in situ tensile strength is about 0.5 MPa (Schultz, 1995), this is a possible mechanism for the formation of T-shaped fractures at contacts (Fig. 15; Zhang et al., 2007) and fracture arrest in heterogeneous fault zones and layered rocks in general.

The deflection of a fracture into a T-shape on meeting a discontinuity such as a fracture or a contact (Figs. 14 and 15) is not limited to discontinuities at right angles to the propagating fracture. In fault zones, the fractures generally show a range in strikes (Fig. 12), suggesting that earlier fractures may be oblique to, and

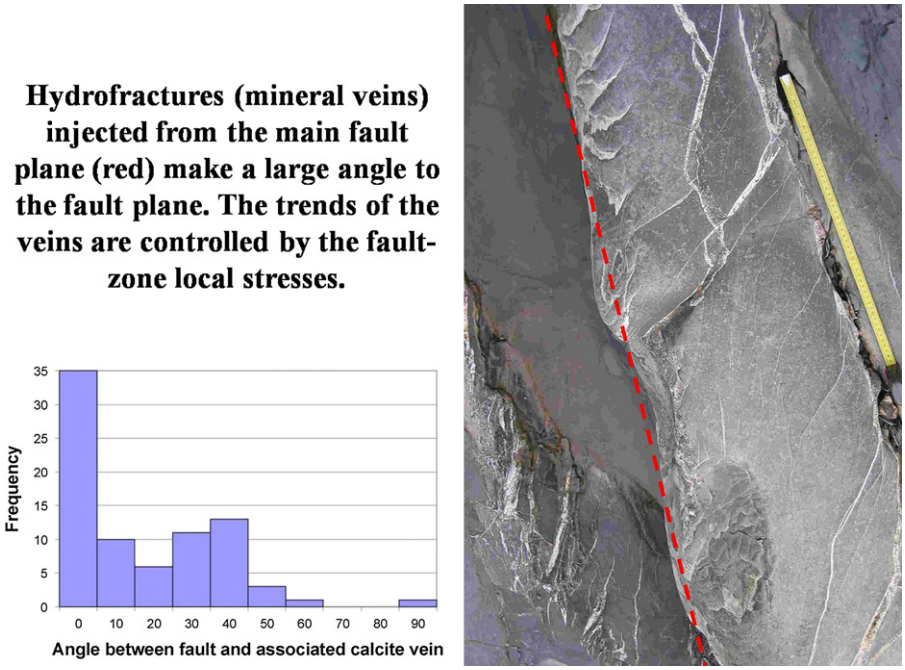

Fig. 12. Many hydrofractures (mineral veins) injected from the main fault plane (broken line) differ in trend from the fault plane. This is shown on the inset histogram, giving the angle between the veins and the fault plane. This indicates that the local stresses in the damage zone, during vein injection, where different from those associated with the fault plane and also that the stiffness variation may have been more irregular with distance than that in the modelled and observed faults zones in Figs. 5 and 8–11. Location: the Bristol Channel at Kilve, the Somerset Coast, England.

contribute to the arrest of, subsequently formed fractures. Also, the various contacts in heterogeneous fault zones will commonly make an angle to a propagating fracture (Fig. 11). This aspect of the Cook–Gordon mechanism is best illustrated through simple numerical models, using the Beasy program (Beasy, 1991; Brebbia and Dominguez, 1992; www.beasy.com) where the weak discontinuity is modelled as an internal spring, that is, a rock layer that behaves as compliant, but still elastic, material (Fig. 9). Some modelling results of an oblique discontinuity deflecting, and presumably arresting, the propagation of fractures are given in Fig. 16.

Experiments on dynamic crack propagation indicate that Cook–Gordon debonding is a common mechanism of fracture deflection and arrest, referred to as delamination in composite materials (Xu et al., 2003; Xu and Rosakis, 2003; Wang and Xu, 2006). The results suggest that it is primarily the tensile strength of the discontinuity itself which determines if the debonding takes place (Wang and Xu, 2006). When the fracture-induced tensile stress has opened up the discontinuity, the propagating fracture, on meeting the discontinuity, may become deflected along the discontinuity (Figs. 14–16), provided the stress field is favourable to such a path change. Experimental results (Xu et al., 2003) support the theoretical results of He and Hutchinson (1989) in that a mode I fracture, such as many mineral veins in fault zones (Fig. 4; Gudmundsson et al., 2002), that becomes deflected into the discontinuity changes into a mixed-mode fracture.

The local stress fields in the layers on either side of a discontinuity or layer contact may also decide whether a propagating fracture becomes deflected on meeting the discontinuity. The local stress change, rotation and change in magnitude of the principal stresses, may happen even if the layers are "welded together" and results in the formation of a barrier to the propagation of fractures of a certain type. Many studies have been made of barriers due to principal-stress rotation in recent years (e.g., Gudmundsson, 2006; Gudmundsson and Brenner, 2004; Faulkner et al., 2006; Gudmundsson and Philipp, 2006). The numerical examples for faults zones provided here (Figs. 7, 10, 11) show that the stress trajectories (directions) of σ_3 (the minimum principal compressive, maximum tensile, stress) and the stress magnitudes inside the fault zone are different from those outside the fault zone and also different between subzones of the damage zone (Figs. 10 and 11). In addition, the contacts between the zones, particularly between the core and the inner damage zone, may be such as to encourage fracture deflection and arrest (Figs. 14–16). Thus, many fractures in the damage zone may become deflected and/or arrested on meeting the contacts between the damage zone and the host rock (Figs. 7 and 10), or between subzones of the damage zone (Figs. 10 and 11), because of properties of the contacts themselves and because of changes in the magnitudes and rotation of the principal stresses.

4.2. Toughness of a discontinuity

The Cook–Gordon and stress rotation (stress barrier) mechanisms cause many fractures in heterogeneous rocks in general, and fault zones in particular, to become deflected and/or arrested at discontinuities and contacts between dissimilar rocks. But the difference in material toughness between the interface/discontinuity/contact and the adjacent rock layers is also of fundamental importance. Generally, material toughness (critical energy release rate) is a measure of the energy needed to propagate a fracture through a material (Hull and Clyne, 1996; Chawla, 1998). Thus, a tough material has a larger area under the stress–strain curve before failure than a brittle material. Material toughness is defined as the energy (in joule) absorbed per unit area of crack. The term "fracture toughness" is sometimes regarded as synonymous with material toughness (Hutchinson, 1996), but "fracture toughness" is mostly used for the critical stress-intensity factor, K_c (Broek, 1978; Karihaloo, 1995). Thus, even if critical stress-intensity factor K_c and the critical strain energy release rate G_c are related and are both a measure of fracture resistance, they have different units and are

Fig. 13. View north, a section of limestone and shale layers in the Bristol Channel in Wales. The joints (extension fractures, many with mineral fillings) differ in trends between the limestone layers, as indicated. For example, where the person is sitting, the joints in the layer at her feet differ by about 20° from those in the next layer above, as indicated by the joint-parallel arrows. Since extension fractures are perpendicular to σ_3 (the minimum principal compressive, maximum tensile, stress), its trend in different limestone layers is likely to have differed by this amount at the time of joint formation.

best regarded as distinct. Here, fracture toughness denotes the critical stress-intensity factor for a crack to propagate, with the units of stress (pascal) times square root of crack length, whereas material toughness has the units of energy per unit area (Kobayashi, 2004; Broberg, 1999; Anderson, 2005; Rice, 2006; Rice and Cocco, 2007).

The total strain energy release rate G_{total} in a mixed-mode fracture propagation is given by:

$$G_{\text{total}} = G_{\text{I}} + G_{\text{II}} + G_{\text{III}} = \frac{(1-\nu^2)K_{\text{I}}^2}{E} + \frac{(1-\nu^2)K_{\text{II}}^2}{E} + \frac{(1+\nu)K_{\text{III}}^2}{E} \tag{2}$$

where $G_{\text{I–III}}$ are the material toughnesses for the ideal crack-displacement modes I–III (Broberg, 1999; Anderson, 2005), E is Young's modulus (compliance or stiffness), ν is Poisson's ratio, and $K_{\text{I–III}}$ are the associated stress-intensity factors. The critical value of the stress-intensity K_{c} denotes the fracture toughness. Eq. (2) assumes plane-strain conditions; in the case of plane-stress, the term $(1-\nu^2)=1$. By their nature and loading, fractures that become deflected into discontinuities or interfaces (contacts) are generally of a mixed-mode (Hutchinson, 1996; Xu et al., 2003).

As regards pure crack-displacements, the opening (extension) mode is denoted by I, the in-plane shear mode by II, and the out-of-plane (anti-plane) shear mode by III (Broberg, 1999; Anderson, 2005). In geology, a mode I crack model is suitable for extension fractures whereas mode II is suitable for many dip-slip faults (normal and reverse) and mode III for strike-slip faults. All of these fracture types and modes, I–III, are common in the damage zones of fault zones (Figs. 3–5).

If the subzones or layers on either side of a discontinuity have the same mechanical properties, such as is sometimes approximately the case in parts of a faults zone, the condition for an extension fracture to penetrate the discontinuity (Fig. 14B) is that the strain energy release rate G_{p}, (with subscript p for penetration) reaches the critical value for fracture extension, namely the material toughness of the layer, Γ_{L} (with subscript L for rock layer). Thus, from Eq. (2) the conditions become:

$$G_{\text{p}} = \frac{(1-\nu^2)K_{\text{I}}^2}{E} = \Gamma_{\text{L}} \tag{3}$$

By contrast, the fracture will kink at or deflect into the discontinuity if the strain energy release rate reaches the material toughness of the discontinuity itself, Γ_{D} (with superscript D for discontinuity). Since the fracture propagates in a mixed-mode (mode I and II) along the discontinuity (Hutchinson, 1996; Xu et al., 2003; Wang and Xu, 2006), it follows from Eq. (2) that deflection into the discontinuity occurs if:

$$G_{\text{d}} = \frac{(1-\nu^2)}{E}\left(K_{\text{I}}^2 + K_{\text{II}}^2\right) = \Gamma_{\text{D}} \tag{4}$$

where the stress-intensity factors $K_{\text{I}} + K_{\text{II}}$ now refer to the discontinuity. From Eqs. (3) and (4), the extension fracture penetrates the discontinuity if:

$$\frac{G_{\text{d}}}{G_{\text{p}}} < \frac{\Gamma_{\text{D}}}{\Gamma_{\text{L}}} \tag{5}$$

but becomes deflected into the discontinuity if:

$$\frac{G_{\text{d}}}{G_{\text{p}}} \geq \frac{\Gamma_{\text{D}}}{\Gamma_{\text{L}}} \tag{6}$$

Equations (3)–(6) are likely to control, partly at least, whether a fracture penetrates or becomes deflected along a discontinuity, such as a fracture or a contact, in some fault zones.

When there is an abrupt change in the mechanical properties at interfaces such as contacts or discontinuities (Figs. 2–5, 8), an elastic mismatch, the assumption of the rock layers on either side of the interface being with the same properties is not warranted. The magnitude of the mechanical change across a discontinuity or an interface is commonly indicated by the Dundurs (1969) elastic mismatch parameters. The two Dundurs parameters, α and β, may be given as (cf. He and Hutchinson, 1989; Hutchinson, 1996; Freund and Suresh, 2003):

$$\alpha = \frac{E_1^* - E_2^*}{E_1^* + E_2^*} \tag{7}$$

$$\beta = \frac{1}{2}\frac{\mu_1(1-2\nu_2) - \mu_2(1-2\nu_1)}{\mu_1(1-\nu_2) + \mu_2(1-\nu_1)} \tag{8}$$

where μ is shear modulus, ν is Poisson's ratio, and the plain strain Young's modulus is $E^* = E/(1-\nu^2)$. The subscript 2 is used for the modulus of the rock hosting the fracture and subscript 1 for the material on the other side (the far side with respect to the fracture tip) of the discontinuity. Generally, α is a measure of mismatch in the extensional or uniaxial stiffness and β in the volumetric or areal stiffness (Freund and Suresh, 2003).

The strain energy release rate associated with fracture penetration into the layer above the discontinuity, G_{p}, is given by (He and Hutchinson, 1989; He et al., 1994):

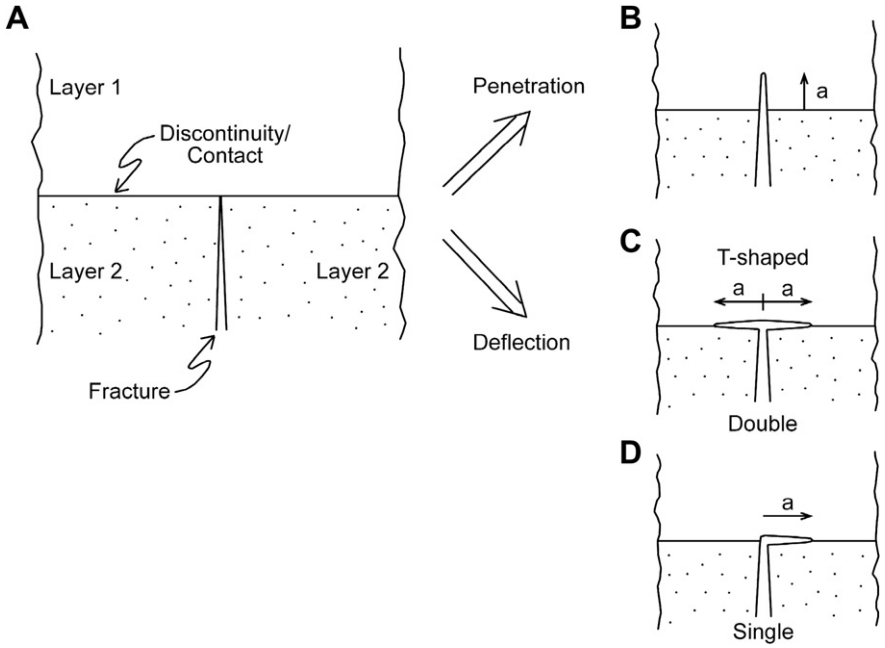

Fig. 14. On meeting an interface or discontinuity such as a contact, a fracture may (A) become arrested, (B) penetrate layer 1 above (or on the other or far side of) the contact, or become doubly (C) or singly (D) deflected into the discontinuity. In case C, the result is a T-shaped fracture (Fig. 15). Modified from Hutchinson (1996).

$$G_p = \frac{1-\nu_1}{2\mu_1} K_I^2 = \frac{1-\nu_1}{2\mu_1} c^2 k_1^2 a^{1-2\lambda} \quad (9)$$

where a is the length of fracture penetration (Fig. 14), k_1 is an amplitude factor, proportional to the loading (here the driving stress or fluid overpressure for fracture propagation), λ is real and c a non-dimensional complex-valued functions, both of which depend on the Dundurs parameters (Eqs. (7) and (8)). The strain energy release rate associated with fracture deflection into the discontinuity or interface, G_d, is given by (He and Hutchinson, 1989; He et al., 1994):

$$G_d = [(1-\nu_1)/\mu_1 + (1-\nu_2)/\mu_2]\left(K_I^2 + K_{II}^2\right) \Big/ \left(4\cos h^2 \pi\varepsilon\right) \quad (10)$$

with

$$K_I^2 + K_{II}^2 = k_1^2 a^{1-2\lambda}\left[|d|^2 + |e|^2 + 2R_e(de)\right] \quad (11)$$

where d and e are non-dimensional complex-valued functions that depend on the Dundurs parameters. The ratio G_d/G_p is independent of k_1 as well as the fracture-segment length a (Fig. 14) and is given by (He and Hutchinson, 1989):

$$\frac{G_d}{G_p} = \frac{1-\beta^2}{1-\alpha} \times \frac{|d|^2 + |e|^2 + 2R_e(de)}{c^2} \quad (12)$$

By analogy with Eqs. (5) and (6), the fracture is likely to penetrate the discontinuity or interface between the dissimilar layers if:

$$\frac{G_d}{G_p} < \frac{\Gamma_D(\psi)}{\Gamma_L^1} \quad (13)$$

but more likely to become deflected into the discontinuity (and often arrested) if:

$$\frac{G_d}{G_p} \geq \frac{\Gamma_D(\psi)}{\Gamma_L^1} \quad (14)$$

the subscript for the material toughness being for layer 1 (Figs. 14 and 17) and ψ is a measure of the relative proportion of mode II to mode I, namely, $\psi = \tan^{-1}(K_{II}/K_I)$ so that $\psi = 0^\circ$ is for pure mode I and $\psi = \pm 90^\circ$ for pure mode II.

For a given fracture-segment length a (Fig. 14), the energy release rate depends on α (assume $\beta = 0$), and the ratio G_d/G_p (Eqs. (12)–(14)) can be plotted as a function of α (Fig. 17). In the area below the curves the ratio G_d/G_p favours deflection of a fracture into the discontinuity, whereas in the area above the curves the ratio

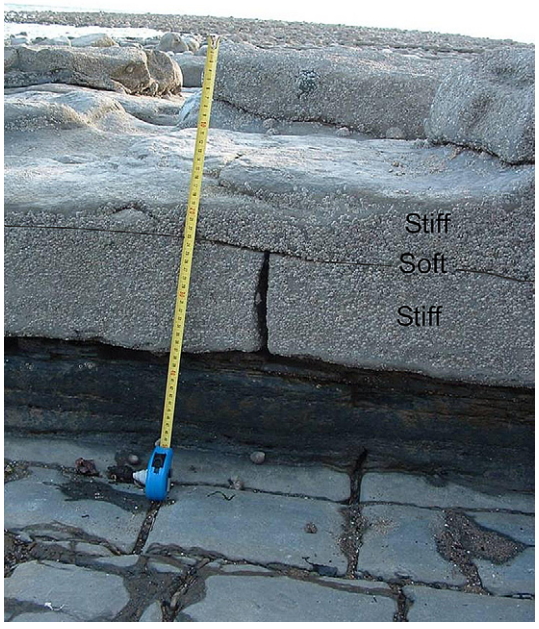

Fig. 15. T-shaped fracture at a contact between soft shale and stiff limestone in the Bristol Channel in Wales. The fracture penetrates the cm-thick soft shale layer and then becomes doubly deflected (Fig. 14) to generate a T-shape.

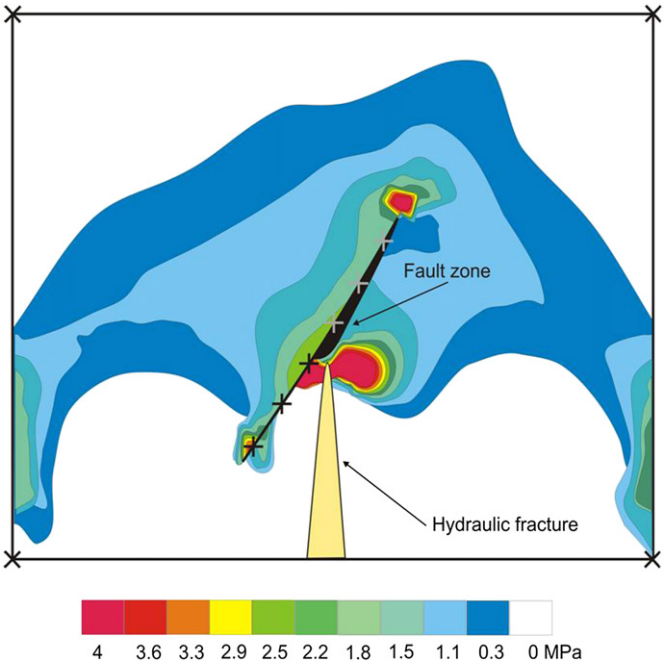

Fig. 16. Boundary-element (Beasy) model of a propagating fracture (here a hydrofracture) meeting with an oblique, weak interface or discontinuity (here a fault zone). These results, showing the (asymmetric) opening and the tensile stresses in megapascals, are completely general. If an extension fracture of any kind meets with a weak interface (for example, a low-tensile strength discontinuity) at an angle, it tends to open up the interface. If the interface trends perpendicular to the propagating extension fracture, the opening is symmetric and may result in a T-shaped fracture (Fig. 15, Gudmundsson, 2003); if the interface is oblique to the advancing extension fracture, the opening is asymmetric, commonly resulting in a singly deflected fracture (Fig. 14D). Fracture propagation inside fault zones, particularly between layers within the damage zone, between the damage zone and the core, and between the damage zone and the host rock may become similarly deflected and, commonly, arrested.

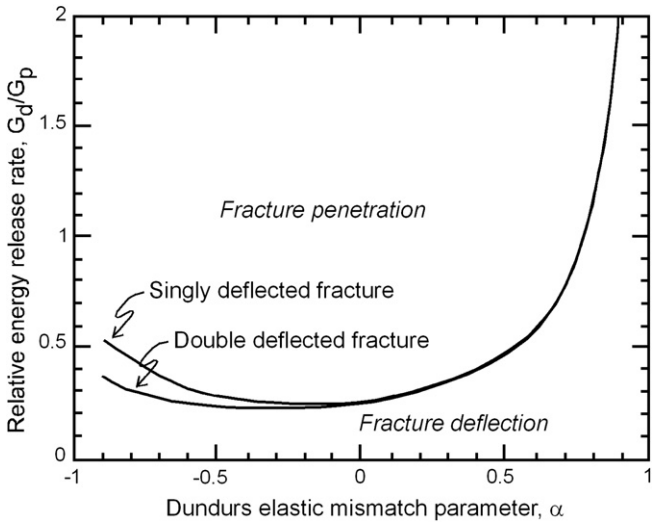

Fig. 17. When a fracture meets an interface, the ratio of strain energy release rate for fracture deflection (G_d) to that of fracture penetration (G_p) controls the fracture propagation. The ratio is here shows as a function of the Dundurs elastic mismatch parameter α (Eqs. (7) and (8)). There is little difference in the elastic strain energy release rate for a single or double deflection (cf. Figs. 14–16). For negative values of α, layer 2 (the fracture-hosting layer) is stiffer than layer 1 and there is little tendency to fracture deflection along the interface. However, as the stiffness of layer 2 decreases in relation to that of layer 1, the tendency to fracture deflection along the interface greatly increases. Modified from He et al. (1994).

favours vertical penetration of the fracture through the discontinuity and into layer 1. Also, when stiffness of layer 1 is equal to that of layer 2, the Dundurs parameter $\alpha = 0$ and $G_d/G_p = 0.26$. Then a fracture deflects along the discontinuity or interface only if the material toughness of the discontinuity (Γ_D) is less than 26% of the material toughness of layer 1 (Γ_L^1). This latter condition is probably uncommon, which may partly explain why fractures tend to penetrate layered rocks, rather than become deflected or arrested at the layer contacts, where all the layers have similar mechanical properties.

Furthermore, the curves in Fig. 17 show that the conditions for a single-directed and a double-directed fracture propagation (a T-shaped fracture, Fig. 15) along the discontinuity are very similar for most values of α. Thus, for practical purposes, the tendency for a fracture to be deflected in one or two directions along the discontinuity may be regarded as the same. When α is negative, that is, the stiffness of layer 1 is less than that of layer 2, there is generally much less tendency for deflection of a fracture along the discontinuity than when α is positive. When the positive value of α increases and layer 1 becomes stiffer in relation to layer 2 (Eq. (8)), there is a greatly increased tendency for a fracture to deflect into the discontinuity.

5. Discussion

One of the principal results of this study is that fractures in fault zones propagate only when and where the local stresses are favourable to that type of fracture propagation (Fig. 18). Because a fault zone is normally very heterogeneous as regards its mechanical properties, the local stresses within the fault zone are also likely to be heterogeneous and change abruptly from one part of the zone to another. In particular, the commonly observed mechanical layering inside a fault zone (Figs. 2–5, 8, 9) is likely to result in local stresses that vary between its subzones (Figs. 10 and 11). It follows that uniform stresses over large parts of the fault zone, a stress field homogenisation (Gudmundsson and Homberg, 1999), which is a necessary condition for the propagation of large fractures or fault slip along large parts of, or the entire, fault zone are rarely reached. This is one reason why most fracture-propagation paths remain short and why most fault slips, both along the

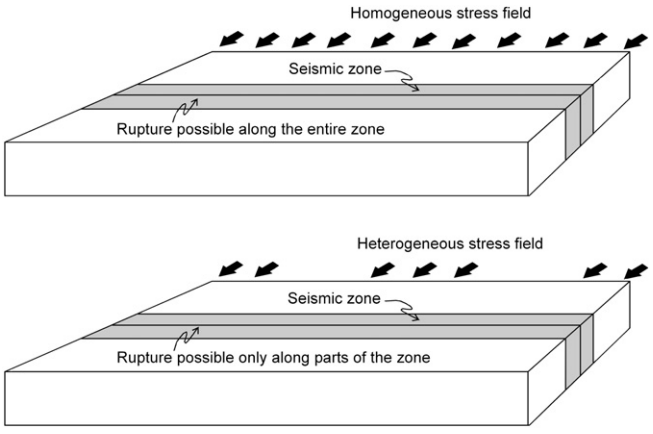

Fig. 18. Fault zone is normally very heterogeneous as regards its mechanical properties, so that its local stresses are likely to be heterogeneous and change abruptly from one part of the zone to another, as indicated schematically in this illustration. Consequently, many fractures in the damage zone become arrested after a short propagation when they enter layers, or meet with interfaces/contacts, that are unfavourable to their propagation.

main fault itself as well as along smaller faults in the damage zone, remain small.

Thus, because of the variations in local stresses and rock properties within fault zones, stress fields favouring a particular type of fracture propagation (for example, an extension fracture) are usually only satisfied within a comparatively small region or rock volume at any one time (Fig. 18). A fracture formed, or slipping, within that region will, as soon as it tries to propagate beyond that region, enter fault zone parts with different properties and, normally, different local stresses. Commonly, these different stresses are unfavourable to that type of fracture propagation (Fig. 18), so that the fracture tends to become deflected and, often, arrested.

One of the principal mechanism by which a propagating fracture becomes deflected and/or arrested at a discontinuity or an interface is through meeting with stress barriers. Such barriers are simply layers or rock units with local stresses that are unfavourable to the propagation of the particular type of fracture. A barrier of this type is primarily generated through rotation and changes in magnitude of the principal stresses in the layer on the far side of an interface or a discontinuity. Many studies have been made of the relevance of this mechanism for fracture deflection and arrest, and all indicate that it is a viable and common mechanism in layered rocks (Gudmundsson, 2006; Gudmundsson and Brenner, 2004; Faulkner et al., 2006; Gudmundsson and Philipp, 2006). The results of the numerical models are supported by numerous field observations (Figs. 13 and 15). This mechanism is doubtless important for fracture deflection and arrest in heterogeneous and layered fault zones, as is indicated by model results (Figs. 7, 10, 11). The mechanism is likely to contribute to fractures in the damage zone becoming deflected and/or arrested on meeting the contacts between the damage zone and the host rock (Figs. 7 and 10), or at contacts between subzones of the damage zone (Figs. 10 and 11).

The conditions for fracture deflection and arrest at interfaces between dissimilar layers, however, depend on two additional factors: first, the mechanical properties of the interface itself in relation to those of the adjacent rocks and, second, on the direction of the fracture propagation in relation to the stiffnesses of the rocks through which it propagates. Analytical solutions (Eqs. (5), (6) and (13), (14)) indicate that the probability of fracture becoming deflected and/or arrested at an interface, rather than penetrating the interface, depend on the ratios between the material toughnesses of the rock layer on the opposite side of the interface and that of the interface itself in relation to the energy release rates associated with fracture deflection and penetration. In particular, when the energy release rate ratio is below certain critical values, deflection into the interface is favoured whereas above those values fracture penetration of the interface and into the layer on the other side of it is favoured (Fig. 17).

Thus, a fracture propagating through a soft pyroclastic or sedimentary layer towards a stiff basaltic lava flow would be more likely to deflect into the discontinuity than a fracture propagating form a stiff lava flow towards a soft pyroclastic layer. This conclusion is supported by many experiments on fracture propagation and arrest at discontinuities between dissimilar layers (Kim et al., 2006), and in geological analogue experiments (Kavanagh et al., 2006). When the deflection is not possible because of the orientation of the principal stresses (Fig. 10), then the fracture propagating from a soft towards a stiff layer would tend to become arrested at the discontinuity. This is exactly what is commonly seen in the field (Figs. 13 and 15), that is, the discontinuity or contact acts as a trap and arrests the fracture propagation.

The analytical results also indicate that a fracture propagating from a layer with a lower Young's modulus towards a layer with a higher Young's modulus has a strong tendency to become deflected along the contact or interface between the layers and, commonly, arrested. By contrast, when the fracture propagates from a high-Young's modulus layer towards a low-Young's modulus layer, the fracture tends to penetrate the contact or interface. These results are supported by materials-science experiments (Kim et al., 2006) and numerous field observations of rock fractures. For example, it is common to see dykes and other rock fractures propagating through relatively compliant (soft) rocks, such as basaltic breccias and other pyroclastic rocks, to be deflected and arrested at contacts with stiffer rocks such as basaltic lava flows (Gudmundsson, 2003).

These results apply equally well to fault zones and suggest that it is more difficult for fractures to propagate from the compliant core into the adjacent subzones of the damage zone (Fig. 12) than from the damage zone into the core. By analogy, it is also easier for fractures coming from the outer, stiffer parts of the damage zone to penetrate the softer inner parts of the damage zone (Figs. 9 and 10) than for fractures propagating in the opposite direction. Also, while fractures may comparatively easily propagate from the host rock into the damage zone, they would tend to become deflected and/or arrested when propagating from the damage zone rock towards the host rock, thereby confining the fault zone thickness at any particular time (Figs. 5–11).

6. Conclusions

The main conclusions of this study may be summarised as follows:

- A fault zone may be regarded as an elastic inclusion with mechanical properties that differ from those of the host rock. The fault zone normally develops its own local stresses which differ from the associated regional stresses.
- The local stresses of the fault zone and its heterogeneities and interfaces and discontinuities (fractures, contacts) to a large extent determine propagation, deflection, and arrest of the fractures in the fault zone.
- Numerical models, provided here, show that the magnitudes and directions of the principal stresses inside a fault zone differ significantly from those in the host rock. For a mechanically layered damage zone, there are abrupt changes in local stresses not only between the core and the damage zone but also between the layers or subzones of the damage zone itself.
- Abrupt changes in local stresses within the fault zone may generate barriers to fracture propagation and contribute to fracture deflection and arrest at interfaces and discontinuities. Arrested (layer-bound) fractures contribute little to permeability development of a fault zone and the associated fluid transport.
- Analytical solutions on the material toughnesses of interfaces such as discontinuities and contacts between mechanically dissimilar layers within a fault zone show that fractures commonly become deflected into, and often arrested at, interfaces.
- Fractures propagating from a softer layer towards a stiffer layer tend to become deflected and/or arrested at the contact between the layers, whereas fractures propagating from a stiff layer towards a soft one tend to penetrate the contact. It is thus normally easier for a fracture to propagate from the damage zone into the soft core than in the opposite direction.
- It is also normally more difficult for a fracture to propagate from the inner, softer parts of the damage zone, to the outer stiffer parts, and from the outer stiffer parts of the damage zone into the host rock, than in the opposite directions.
- Fracture propagation, deflection, and arrest at interfaces and, alternatively, penetration of the interfaces, have large effects

on how fault damage zones and cores grow and change their permeability and mechanical structure with time.

Acknowledgements

We thank Isabel Bivour, Gabriele Ertl, Oktawian Ewiak, Sonja Geilert, and Kristine Nilsen for running some of the numerical models and for help with the figures and the reviewers, Valerio Acocella and Derek Keir, for very helpful comments. This work was supported by the Norwegian Research Council Petromaks project no. 163316/S30 "Carbonate Reservoir Geomodels".

References

Agosta, F., Aydin, A., 2006. Architecture and deformation mechanism of a basin-bounding normal fault in Mesozoic platform carbonates, central Italy. J. Struct. Geol. 28, 1445–1467.
Ahlbom, K., Smellie, J.A.T., 1991. Overview of the fracture zone project at Finnsjön. Sweden J. Hydrol. 126, 1–15.
Amadei, B., Stephansson, O., 1997. Rock Stress and its Measurement. Chapman & Hall, London.
Anderson, T.L., 2005. Fracture Mechanics: Fundamentals and Applications, third ed. Taylor & Francis, London.
Barton, C.A., Zoback, M.D., Moos, D., 1995. Fluid flow along potentially active faults in crystalline rock. Geology 23, 683–686.
Beasy, 1991. The Boundary Element Analysis System User Guide. Computational Mechanics, Boston.
Bell, F.G., 2000. Engineering Properties of Soils and Rocks, fourth ed. Blackwell, Oxford.
Berg, S.S., Skar, T., 2005. Controls on damage zone asymmetry of a normal fault zone: outcrop analyses of a segment of the Moab fault, SE Utah. J. Struct. Geol. 27, 1803–1822.
Braathen, A., Berg, S.S., Storro, G., Jaeger, O., Henriksen, H. and Gabrielsen, R., 1999. Fracture-zone geometry and groundwater flow; results from fracture studies and drill tests in Sunnfjord. Geological Survey of Norway, Report 99.017, 68 pp. (in Norwegian).
Bradbury, K.K., Barton, D.C., Solum, J.G., Draper, S.D., Evans, J.P., 2007. Mineralogical and textural analyses of drill cuttings from the San Andreas Fault Observatory (SAFOD) boreholes: initial interpretations of fault zone composition and constraints on geologic models. Geosphere 3, 299–318.
Brebbia, C.A., Dominguez, J., 1992. Boundary Elements: An Introductory Course. Computational Mechanics, Boston.
Bredehoeft, J.D., 1997. Fault permeability near Yucca Mountain. Water Resour. Res. 33, 2459–2463.
Broberg, K.B., 1999. Cracks and Fracture. Academic Press, New York.
Broek, D., 1978. Elementary Fracture Mechanics, second ed. Nordhoff, Leiden.
Bruhn, R.L., Parry, W.T., Yonkee, W.A., Thompson, T., 1994. Fracturing and hydrothermal alteration in normal fault zones. Pure Appl. Geophys. 142, 609–644.
Byerlee, J., 1993. Model for episodic flow of high-pressure water in fault zones before earthquakes. Geology 21, 303–306.
Caine, J.S., Evans, J.P., Forster, C.B., 1996. Fault zone architecture and permeability structure. Geology 24, 1025–1028.
Chawla, K.K., 1998. Composite Materials: Science and Engineering, second ed. Springer, Berlin.
Cook, J., Gordon, J.E., 1964. A mechanism for the control of crack propagation in all-brittle systems. Proc. R. Soc. Lond., Ser. A282, 508–520.
Dundurs, J., 1969. Edge-bonded dissimilar orthogonal wedges. J. Appl. Mech. 36, 650–652.
Eshelby, J.D., 1957. The determination of the elastic field of an ellipsoidal inclusion, and related problems. Proc. R. Soc. Lond. A241, 376–396.
Evans, J.P., Forster, C.B., Goddard, J.V., 1997. Permeability of fault-related rocks, and implications for hydraulic structure of fault zones. J. Struct. Geol. 19, 1393–1404.
Farmer, I., 1983. Engineering Behaviour of Rocks, second ed. Chapman and Hall, London.
Faulkner, D.R., Mitchell, T.M., Healy, D., Heap, M.J., 2006. Slip on "weak" faults by the rotation of regional stress in the fracture damage zone. Nature 444, 922–925.
Fisher, A.T., Zwart, G., Ocean Drilling Program Leg 156 Scientific Party, 1996. Relation between permeability and effective stress along a plate-boundary fault, Barbados accretionary complex. Geology 24, 307–310.
Freund, L.B., Suresh, S., 2003. Thin Film Materials: Stress, Defect Formation and Surface Evolution. CUP, Cambridge.
Gudmundsson, A., 2000. Active fault zones and groundwater flow. Geophys. Res. Lett. 27, 2993–2996.
Gudmundsson, A., 2003. Surface stresses associated with arrested dykes in rift zones. Bull. Volcanol. 65, 606–619.
Gudmundsson, A., 2004. Effects of Young's modulus on fault displacement. C.R. Geosci. 336, 85–92.
Gudmundsson, A., 2006. How local stresses control magma-chamber ruptures, dyke injections, and eruptions in composite volcanoes. Earth Sci. Rev. 79, 1–31.
Gudmundsson, A., 2007. Infrastructure and evolution of ocean-ridge discontinuities in Iceland. J. Geodyn. 43, 6–29.
Gudmundsson, A., Brenner, S.L., 2003. Loading of a seismic zone to failure deforms nearby volcanoes: a new earthquake precursor. Terra Nova 15, 187–193.
Gudmundsson, A., Brenner, S.L., 2004. How mechanical layering affects local stresses, unrests, and eruptions of volcanoes. Geophys. Res. Lett. 31. doi:10.1029/2004GL020083.
Gudmundsson, A., Homberg, C., 1999. Evolution of stress fields and faulting in seismic zones. Pure Appl. Geophys. 154, 257–280.
Gudmundsson, A., Philipp, S.L., 2006. How local stress fields prevent volcanic eruptions. J. Volcanol. Geotherm. Res. 158, 257–268.
Gudmundsson, A., Fjeldskaar, I., Brenner, S.L., 2002. Propagation pathways and fluid transport of hydrofractures in jointed and layered rocks in geothermal fields. J. Volcanol. Geotherm. Res. 116, 257–278.
Gutmanis, J.C., Lanyon, G.W., Wynn, T.J., Watson, C.R., 1998. Fluid flow in faults: a study of fault hydrogeology in Triassic sandstone and Ordovician volcaniclastic rocks at Sellafield, north-west England. Proc. Yorkshire Geol. Soc. 52, 159–175.
Haimson, B.C., Rummel, F., 1982. Hydrofracturing stress measurements in the Iceland research drilling project drill hole at Reydarfjordur. Iceland J. Geophys. Res. 87, 6631–6649.
He, M.Y., Hutchinson, J.W., 1989. Crack deflection at an interface between dissimilar elastic materials. Int. J. Solids Struct. 25, 1053–1067.
He, M.Y., Evans, A.G., Hutchinson, J.W., 1994. Crack deflection at an interface between dissimilar elastic materials: role of residual stresses. Int. J. Solids Struct. 31, 3443–3455.
Healy, D., 2008. Damage patterns, stress rotations and pore fluid pressure in strike-slip fault zones. J. Geophys. Res. 113, B12407.
Hicks, E.C., 1996. Crustal Stresses in Norway and Surrounding Areas as Derived from Focal Mechanisms Solutions and in situ Stress Measurements. Cand. Scient. Thesis, University of Oslo, Oslo.
Hoek, E., 2000. Practical Rock Engineering. http://www.rockscience.com.
Hull, D., Clyne, T.W., 1996. An Introduction to Composite Materials, second ed. CUP, Cambridge.
Hutchinson, J.W., 1996. Stresses and Failure Modes in Thin Films and Multilayers. Notes for a Dcamm Course. Technical University of Denmark, Lyngby, pp. 1–45.
Jaeger, J.C., Cook, N.G.W., Zimmerman, R.W., 2007. Fundamentals of Rock Mechanics, fourth ed. Blackwell, Oxford.
Karihaloo, B.L., 1995. Fracture Mechanics and Structural Concrete. Longman, Brunt Mill, Harlow, UK.
Kasahara, K., 1981. Earthquake Mechanics. CUP, Cambridge.
Kavanagh, J.L., Menand, T., Sparks, R.S.J., 2006. An experimental investigation of sill formation and propagation in layered elastic media. Earth Planet. Sci. Lett. 245, 799–813.
Kim, J.W., Bhowmick, S., Hermann, I., Lawn, B.R., 2006. Transverse fracture of brittle bilayers: relevance to failure of all-ceramic dental crowns. J. Biomed. Materials Res. 79B, 58–65.
Kobayashi, T., 2004. Strength and Toughness of Materials. Springer, Berlin.
Larsen, B., 2002. Fracture systems, active faults and groundwater potential on the island of Bømlo, West Norway. MSc thesis, University of Bergen, Bergen, 150 pp. (in Norwegian).
Li, Y.G., Malin, P.E., 2008. San Andreas Fault damage at SAFOD viewed with fault-guided waves. Geophys. Res. Lett. 35, L08304.
Lin, A., Maruyama, T., Kobayashi, K., 2007. Tectonic implications of damage zone-related fault-fracture networks revealed in drill core through the Nojima fault, Japan. Tectonophysics 443, 161–173.
Lopez, D.L., Smith, L., 1995. Fluid flow in fault zones: analysis of the interplay between convective circulation and topographically driven groundwater flow. Water Resour. Res. 31, 1489–1503.
Nativ, R., Adar, E.M., Becker, A., 1999. Designing a monitoring network for contaminated ground water in fractured chalk. Ground Water 37, 38–47.
Nemat-Nasser, S., Hori, M., 1999. Micromechanics: Overall Properties of Heterogeneous Materials, second ed. Elsevier, Amsterdam.
Nilsen, B., Palmström, A., 2000. Engineering Geology and Rock Engineering. Norwegian Soil and Rock Engineering Association (NJFF), Oslo.
Press, F., 1965. Displacements, strains, and tilts at teleseismic distances. J. Geophys. Res. 70, 2395–2412.
Priest, S.D., 1993. Discontinuity Analysis for Rock Engineering. Chapman and Hall, London.
Qu, J., Cherkaoui, M., 2006. Fundamentals of Micromechanics of Solids. Wiley, NJ.
Rice, J.R., 2006. Heating and weakening of faults during earthquake slip. J. Geophys. Res. 111, B05311.
Rice, J.R., Cocco, M., 2007. Seismic fault rheology and earthquake dynamics. In: Handy, M.R., Hirth, G., Horius, N. (Eds.), Tectonic Faults: Agents of Chance on a Dynamic Earth. The MIT Press, Cambridge, MA, pp. 99–137.
Sadd, M.H., 2005. Elasticity: Theory, Applications, and Numerics. Elsevier, Amsterdam.
Savin, G.N., 1961. Stress Concentration Around Holes. Pergamon, New York.
Scholz, C.H., 1990. The Mechanics of Earthquakes and Faulting. CUP, New York.
Schon, J.H., 2004. Physical Properties of Rocks: Fundamentals and Principles of Petrophysics. Elsevier, Oxford.
Schultz, R.A., 1995. Limits on strength and deformation properties of jointed basaltic rock masses. Rock Mech. Rock Eng. 28, 1–15.
Seront, B., Wong, T.F., Caine, J.S., Forster, C.B., Bruhn, R.L., 1998. Laboratory characterisation of hydromechanical properties of a seismogenic normal fault system. J. Struct. Geol. 20, 865–881.
Shimamoto, T., Noda, H., Tanikawa, W., Wibberley, C.A.J., Uehara, S., 2004. Fault-zone permeability structures and their implications for earthquake

mechanisms and geo-engineering problems. In: Ohnishi, Y., Aoki, K. (Eds.), Contributions of Rock Mechanics to the New Century. Millpress Science, Rotterdam, pp. 1021–1026.
Shimada, M., 2000. Mechanical Behavior of Rocks Under High Pressure Conditions. Balkema, Rotterdam.
Sibson, R.H., 1996. Structural permeability of fluid-driven fault-fracture meshes. J. Struct. Geol. 18, 1031–1042.
Sibson, R.H., 2003. Thickness of the seismic slip zone. Geol. Soc. Am. Bull. 93, 1169–1178.
Simmenes, T.H., 2002. Fracture systems: Fault development and fluid transport in Vaksdal, West Norway. MSc thesis, University of Bergen, Bergen, 143 pp.
Steketee, J.A., 1958. Some geophysical applications of the elasticity theory of dislocations. Can. J. Phys. 36, 1168–1198.
Sutton, A.P., Balluffi, R.W., 1995. Interfaces in Crystalline Materials. OUP, Oxford.
Tanaka, H., Omura, K., Matsuda, T., Ikeda, R., Kobayashi, K., Murakamai, M., Shimada, K., 2007. Architectural evolution of the Nojima fault and identification of the activated slip layer by Kobe earthquake. J. Geophys. Res. 112, B07304.
Thouless, M.D., Parmigiani, J.P., 2007. Mixed-mode cohesive-zone models for delamination and deflection in composites. In: Sørensen, B.F., Mikkelson, L.P., Lilhot, H., Goutianos, S., Abdul-Mahdi, F.S. (Eds.), Proceedings of the 28th Risø International Symposium on Material Science: Interface Design of Polymer matrix Composites, pp. 93–111. Roskilde, Denmark.
Wang, P., Xu, L.R., 2006. Dynamic interfacial debonding initiation induced by an incident crack. Int. J. Solids Struct. 43, 6535–6550.
Xu, L.R., Rosakis, A.J., 2003. An experimental study of impact-induced failure events in homogeneous layered materials using dynamic photoelasticity and high-speed photography. Optic Laser Eng. 40, 263–288.
Xu, L.R., Huang, Y.Y., Rosakis, A.J., 2003. Dynamics crack deflection and penetration at interfaces in homogeneous materials: experimental studies and model predictions. J. Mech. Phys. Solids 51, 461–486.
Zhang, X., Jeffrey, R.G., Thiercelin, M., 2007. Deflection and propagation of fluid-driven fractures at frictional bedding interfaces: a numerical investigation. J. Struct. Geol. 29, 396–410.
Zienkiewicz, O.C., 1977. The Finite Element Method. McGraw-Hill, New York.